

Application of Computed X-Ray Tomography Scanning in the Study of Thermo-Oxidative Degradation of Thick-Walled Filled Natural Rubber Vulcanizates

H. LAVEBRATT,*¹ E. ÖSTMAN,² S. PERSSON,² and B. STENBERG¹

¹Department of Polymer Technology, Royal Institute of Technology, S-100 44 Stockholm, Sweden and

²SKEGA AB, S-934 02 Ersmark, Sweden

SYNOPSIS

The aging of five thick-walled natural rubber compounds has been studied by computed X-ray tomography scanning and crosslink density measurements. The compounds were compounded as ordinary carbon-black-filled rubbers with sulfur and peroxide as curing agents. The rubber samples were aged in air at 70, 100, and 150°C for 1000 h. The relatively new technique of computed X-ray tomography scanning proved to be a good method for studying the aging procedure, and especially for following the crack propagation in the surface. Antioxidants (TMQ and 6PPD) had a low effect on the resistance toward oxidative degradation and crosslinking under these conditions. Surprisingly, the efficient sulfur-vulcanized material had a poor resistance toward thermal degradation. When the crosslink density and the computed X-ray tomography scanning results were compared, it was assumed that the computed X-ray tomograph detected oxygen in the surface, both as elementary oxygen and as oxygen in degradation products, i.e., in carbonyls. The results agree well with the theory that oxidative aging is limited by the ability of the oxygen to diffuse into the material.

INTRODUCTION

It is well known that rubber exposed to air undergoes oxidative aging, i.e., chain scission and oxidative crosslinking, resulting in a deterioration in physical properties. Since the rate of oxidative aging is oxygen diffusion controlled, thin rubber components are more affected by oxidative aging than are thick-walled components. When a thick-walled rubber specimen is aged at elevated temperatures, however, the network in the bulk may be degraded if the vulcanizing system has a poor thermal stability.¹

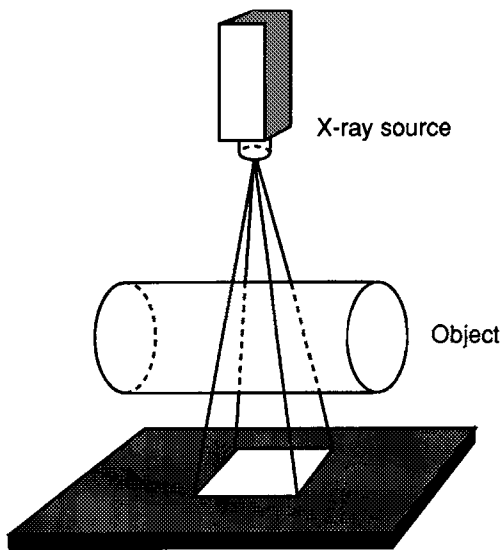
An increase in crosslink density will, according to Mason,² lead to a decrease in specific volume. Gillen³ claimed that there will at the same time be a density increase during aging because of the complex system of gaseous products formed and released during aging, covalently bonded oxygen in the sur-

face, and a volume decrease because of evaporation. He showed by density profiling of an air-aged NBR sample that there is a pronounced density gradient with the highest density at the surface.

In 1971, Hounsfield⁴ and Cormack^{5,6} introduced computed X-ray tomography scanning (CT) as a powerful method of medical diagnosis. The technique was until the late 1970s used solely as a medical tool. Today, CT is a nondestructive testing method for process control in many industries, e.g., the aircraft and nuclear power industries. Persson⁷ has in an earlier work described how the crosslink density in nonfilled peroxide-cured poly(isoprene) rubber can be described by CT. Computed X-ray tomography scanning (derived from the Greek word for slice, *tomos*) has two great advantages over conventional radiography. Above all, tomography provides a distortion-free two-dimensional image of a two-dimensional cross section through an object. Conventional radiography gives, contrarily, a distorted two-dimensional image of a three-dimensional object (Fig. 1). Using CT, a three-dimensional

* To whom correspondence should be addressed.

Conventional radiography



Computed X-ray tomography scanning

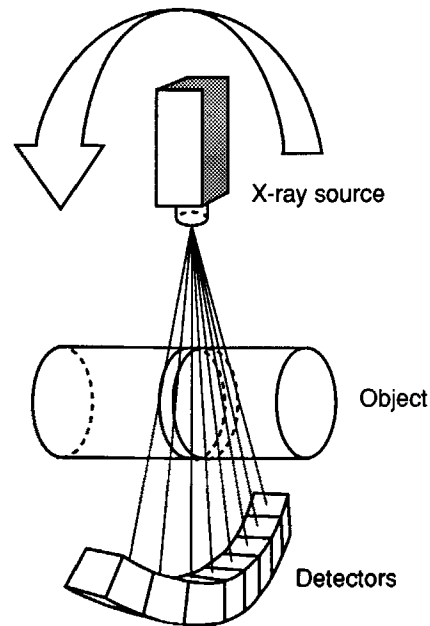


Figure 1 Diagram describing the principal difference between conventional radiography and computed X-ray tomography scanning.

image can be constructed from a series of the two-dimensional tomographs.

Medical CT scanners are able to detect⁸ all materials built of elements with an atomic number lower than 20 (Ca), or with densities less than approximately 2 g/cm³. The linear attenuation coefficient, μ , of the material is represented in CT by the Hounsfield unit (H), also called the CT number, which is related to Hounsfield's own scanner, the EMI mark I. The CT number of a substance with linear attenuation μ_x is defined by the following:

$$\begin{aligned} \text{CT}_{\text{number}} &= 1000 \times \frac{\mu_x - \mu_{\text{water at 73 keV}}}{\mu_{\text{water at 73 keV}}} \\ &= 5263 \times \mu_x - 1000 \quad (1) \end{aligned}$$

From Eq. (1) a CT number of water equal to zero Hounsfield unit can be derived. The CT number of air is -1000 H and that of dense bone $+3095$ H, i.e., the Hounsfield scale ranges over 4096 H values, which can be individually assigned to each picture element. CT makes it possible to study not only the linear attenuation of a material but also the specific weight, thanks to the linear relationship between μ and ρ . A scanner has three essential components; viz., an X-ray source, several detectors, and a com-

puter. During scanning, the X-ray source and the detectors revolve 360° around the object, and the linear attenuation of the X-ray beams in each volume element is measured. A tomographic image is reconstructed from the X-ray intensity measurements. The image is composed of a number of picture elements (pixels), often 512×512 . The CT number of each pixel represents the linear attenuation of the corresponding voxel (volume element) in the actual slice. Due to the statistical variation in the X-ray intensity, μ will have a standard deviation of typically 1–5%. This is an improvement of at least two orders of magnitude over the contrast resolution in conventional radiography. This is the second great advantage of CT. Persson⁷ has shown that a modern CT is able to detect a density difference of approximately 3 mg/cm³. The spatial resolution has in practice been shown not to be the pixel size, but approximately 1.5 times larger than the pixel size.

The aim of this study was to evaluate the possibility of using computed X-ray tomography scanning to study the aging of rubber. For this purpose five thick-walled carbon-black-filled natural rubber vulcanizates were aged at elevated temperatures in air. Aging gradients were determined and compared by computed X-ray tomography scanning and crosslink density measurements.

Table I Formulations in Weight Proportions (phr)

Material Vulcanization system	Conventional			EV	Peroxide
	A1	A2	A3	D	E
SMR CV60	100	100	100	100	100
ISAF N220	45	45	45	45	45
Dutrex 729HP ^a	8	8	8	8	8
ZnO	4	4	4	4	4
Stearic acid	1	1	1	1	1
TMQ ^b	—	3	—	—	—
6PPD ^c	—	—	3	—	—
Antilux 654 ^d	2	2	2	2	2
CBS ^e	0.8	0.8	0.8	1	—
Sulfur	2	2	2	—	—
TMTD ^f	—	—	—	1	—
DTDM ^g	—	—	—	1	—
Di Cup 40 ^h	—	—	—	—	5
Vulcanization temperature	160	160	160	160	160 (°C)
Vulcanization time	80	80	80	80	150 (min)

^a Aromatic, heavy hydrocarbon oil (Shell).

^b Polymerized 1,2-dihydro-2,2,4-trimethylquinoline.

^c *N*-phenyl-*n*'(1,3-dimethylbutyl)*p*-phenyldiamine.

^d Paraffinic hydrocarbon wax (Rhein Chemie).

^e *N*-cyclohexyl-2-benzothiazole sulphenamide.

^f Tetramethylthiuram disulphide.

^g 4,4'-dithiomorpholine.

^h Dicumyl peroxide, 39.5–41.5% active dicumylperoxide supported on precipitated calcium carbonate (Hercules).

EXPERIMENTAL

Materials

The rubber used in this experiment was compounded as an ordinary carbon-black-filled natural rubber. The recipes are shown in Table I. Three traditional curing systems and two antioxidants gave five different compounds; A1 was conventionally sulfur cured by S/CBS, A2 was also cured by S/CBS but contained the antioxidant TMQ, A3 was also cured by S/CBS, but the antioxidant in this case was 6PPD, D was cured by an efficient vulcanization system (TMTD), and the fifth compound E by a peroxide curing system. The compounds were compression molded to cylindrical test pieces with a diameter of 75 mm and a length of 200 mm.

Aging Conditions

The samples were aged at 70, 100, and 150°C in ovens with circulating air. For each combination of material and temperature, two cylinders were manufactured; one for crosslink density measurements and one for CT measurements. At the predetermined

aging times of 0, 1, 4, 9, 17, 28, and 42 days, the cylinders were taken from the ovens for measurement, and then put back into the ovens for continued aging.

Crosslink Density

At each aging time a small cylinder (diameter 10 mm) was drilled from each "crosslink density cylinder." This was done along a diameter (Fig. 2). The hole in the cylinder was plugged with a rubber stopper to protect the interior of the specimen from oxygen attack via these holes. Half the smaller cylinder was then cut into 2-mm-thick slices, the swellability of which in dichloromethane was determined at room temperature ($\chi = 0.525$).⁹ The value of the polymer-solvent interaction parameter χ may, however, be influenced due to oxidation.¹ The crosslink density was calculated according to the well-known Flory-Rehner equation.¹⁰ The influence of carbon black on the crosslink density was compensated for by applying values of the interaction constant suggested by Porter.¹¹

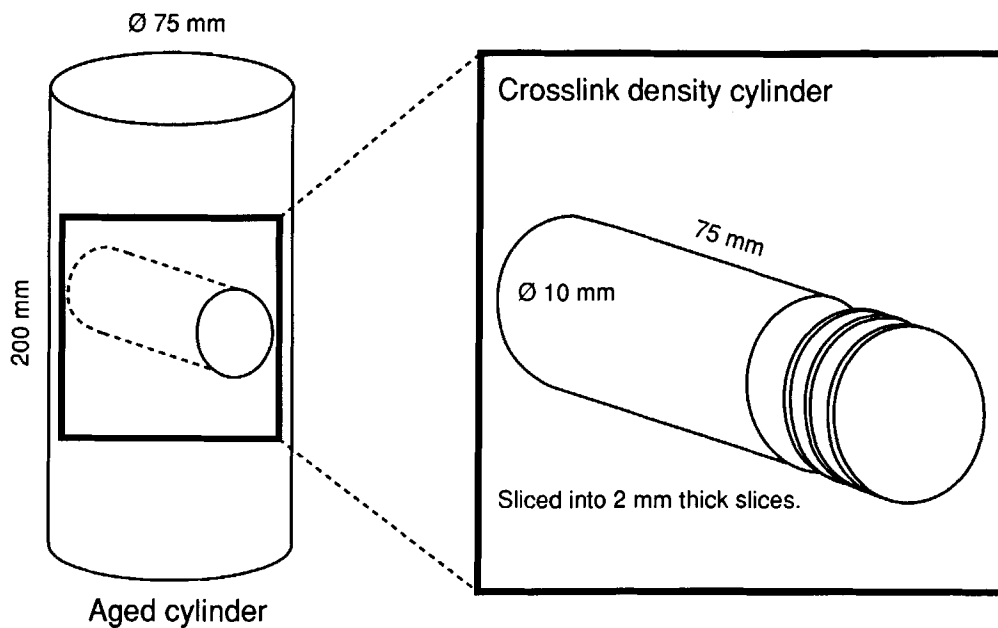


Figure 2 Diagram describing the preparation of crosslink density samples.

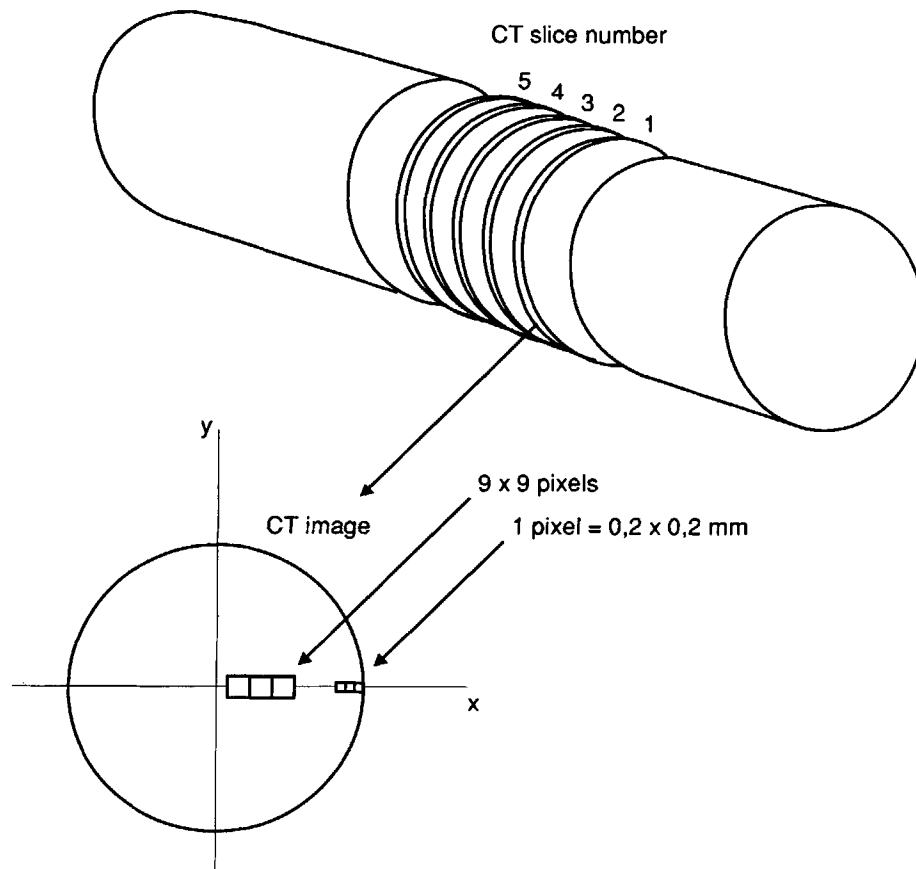


Figure 3 Diagram describing how the CT numbers were measured in the CT images.

Table II Crosslink Density^a in Bulk

Aging Temperature	70°C		100°C		150°C	
	0	1000	0	1000	0	1000
Crosslink Density (10 ⁻⁵ mol cm ⁻³)						
Material						
A1	3.9	5.0	4.1	5.1	4.3	5.8
A2	2.8	3.5	2.1	3.8	3.4	4.5
A3	2.6	3.5	2.8	3.7	2.6	4.4
D	8.5	9.2	8.3	9.8	8.7	2.6
E	10.1	9.4	10.0	10.4	10.1	8.6

^a Mean value of five consecutive slices between 20 and 30 mm into the bulk.

Computed X-Ray Tomography Scanning

The CT measurements were performed at the hospital in Skellefteå using a General Electric 9800 Quick CT scanner. To avoid artifacts arising from the abrupt density change at the edge of the rubber cylinder, the specimen was placed in a water-filled PMMA container during scanning. In each test five consecutive CT slices with a thickness of 10 mm were scanned through the cylinder. Since CT is a nondestructive method, exactly the same region was measured at each aging time (a PTFE thread was inserted in each cylinder surface to provide a starting point for the scans). In each CT slice was the CT-number measured pixel for pixel (1 pixel = 0.2 × 0.2 mm) at the surface and in regions of 9 × 9 pixels along the radius (Fig. 3).

The machine settings during the experiments were

X-ray tube voltage, 140 kV	Anode current, 170 mA
Scan time, 8 s	Scan space, 10 mm
Slice thickness, 10 mm	Scan field of view, large
Filter algorithm, tissue	Matrix size, 512 × 512 pixels

RESULTS

In Table II crosslink densities near the center of the cylinder are shown for samples unaged and aged for 1000 h. Some results, especially those for the EV system (D) at 150°C are very interesting. In this case the crosslink density was lowered to a third of the original, whereas the crosslink density in the conventionally vulcanized materials, A1, A2, and A3, increased 26, 24, and 41%, respectively. Table II also

shows the initial homogeneity of the crosslink density in cylinders of the same material.

Figures 4(a) to 6(b) compare the CT results with the crosslink density results, the results being plotted as a function of the square root of aging time at 100 and 150°C. In the conventional systems both the crosslink density and the CT number increases with time. However, when aging the EV system and the peroxide system at 100°C, the CT number increase whereas the crosslink density decreases.

Figure 7 illustrates how the crosslink density through the cross section of material D changed when the material was aged at 150°C at three aging times. At the surface the crosslink density increased, whereas the bulk showed a distinct degradation.

The thickness of the oxidized layers are shown in Table III. The thickness was evaluated by CT measurements by taking as the oxidized layer the area at the surface where the CT number was higher than in the bulk. Figure 8 shows an area with lower CT number close to the oxidized layer in sample A1 aged at 100°C.

Photographs of CT images shown in Figures 9(a) to 9(d) indicate the increased amount of aged rubber with increased time and the propagating cracks. The material is the peroxide-cured cylinder aged at 150°C. Figure 10 is a three-dimensional CT image of the same material at 42 days aging time, giving a hint of the spread of the oxidized material.

DISCUSSION

Materials A1, A2, and A3 showed aging behavior resembling each other [cf. Figs. 4(a), (b) and 5(a), (b)], although A2 and A3 contained antioxidants. The antioxidants seemed therefore to have little effect on the aging. It is known¹² that conventional antioxidants used in CBS-sulfur systems do not act as well as they ought to do.

The bulk of the A materials showed a slight post-vulcanization, i.e., crosslinking with remaining elementary sulfur, to approximately the same extent at all temperatures (see Table II). This is noteworthy especially at 150°C, where thermal degradation should in general dominate, but desulfuration¹³ is possible, i.e., S_x- and S₂ crosslinks can be broken and will, if the accelerator is still active, be rearranged to monosulfidic crosslinks. The surface of the samples also showed this behavior when aged at 70°C.

The surfaces of the samples aged at 100 and 150°C exhibited crosslink density changes probably dom-

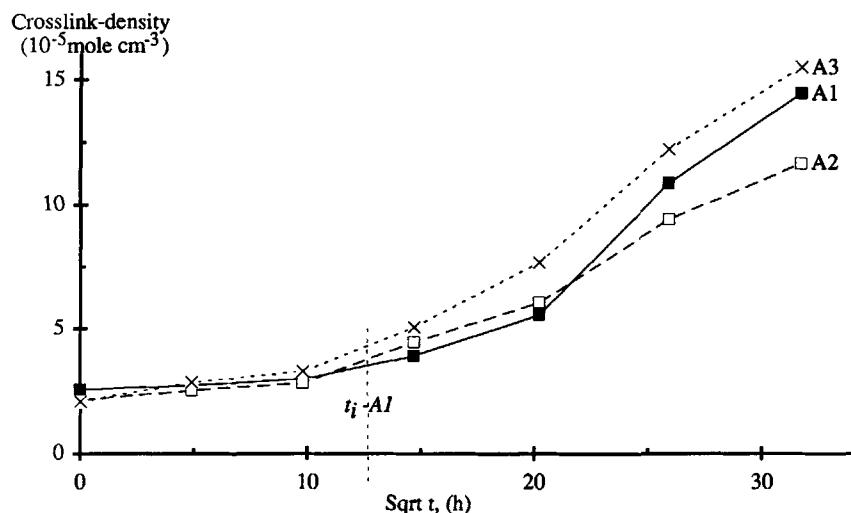


Figure 4(a) Crosslink density of the surface versus the square root of aging time. Materials A1, A2, and A3 aged at 100°C. t_i -A1 denotes the proposed induction time for oxidative crosslinking.

inated by oxidative crosslinking. The CT measurements showed a density increase with a similar trend as the crosslink density [see Figures 4(a), (b) and 5(a), (b)], indicating that the CT number was proportional to crosslink density.

For materials D and E in Figures 6(a) and 6(b), the relation between CT number and crosslink density is unclear. At 100°C the CT number increased whereas the crosslink density decreased because of thermal degradation of the network. A comparison with Persson's work,⁷ showed that the crosslink density changes in this work were too small to be detectable with CT. There appeared therefore to be

other effects than crosslinking leading to a higher density in the surface. This can probably be explained by diffusion of oxygen leading to a density increase. In other words the CT measurements probably detect the amount of diffused oxygen, whether as elementary oxygen or/and as oxygen bound in oxidation products (carbonyl compounds¹³) in a thick-walled unfilled TMTD-vulcanized natural rubber compound with aging has been shown in another publication from this department.¹⁴

The diffusion theory for polymeric materials predicts that the absorption of matter is proportional

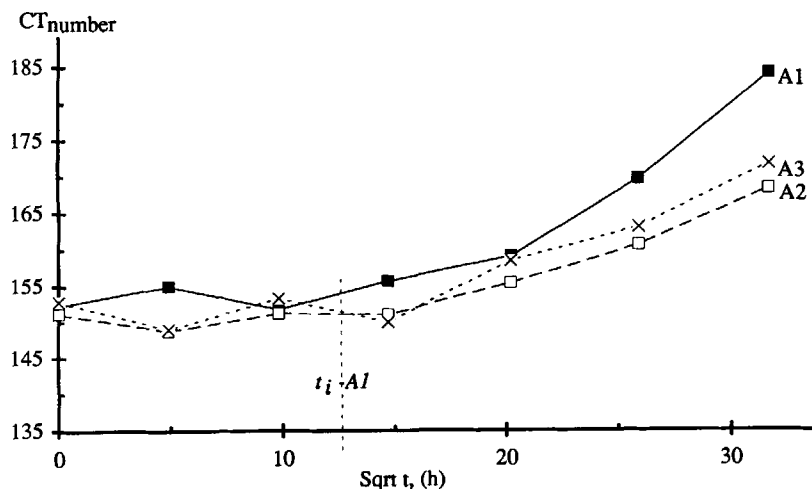


Figure 4(b) CT number of the surface versus the square root of aging time. Materials A1, A2, and A3 aged at 100°C. t_i -A1 denotes the proposed induction time for oxidative crosslinking.

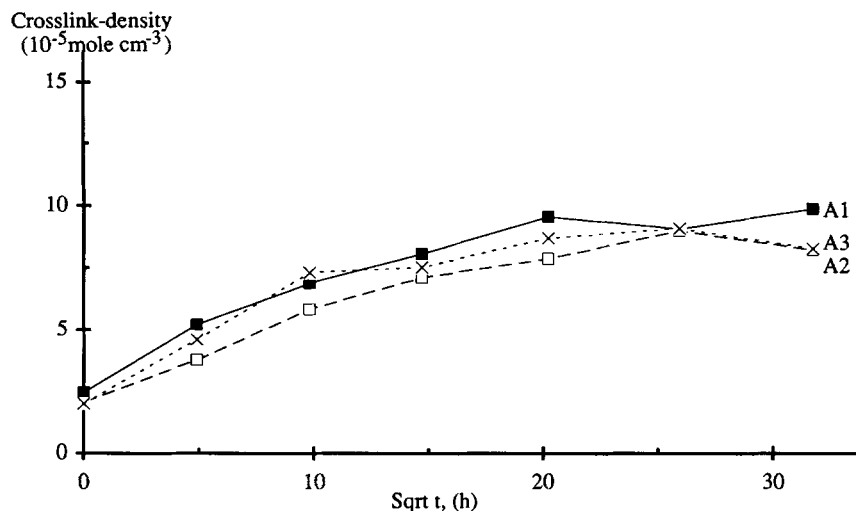


Figure 5(a) Crosslink density of the surface versus the square root of aging time. Materials A1, A2, and A3 aged at 150°C.

to the square root of time.¹⁵ One might therefore expect that the CT curves should be straight lines, but as the aging proceeds, the oxidized layer at the surface lowers the diffusion constant for oxygen, giving a self-limiting aging according to Clough and Gillen¹⁶ and Stenberg et al.¹⁷ They presented measurements of the diffusion rate of oxygen in aged rubber materials and showed a dramatic decrease of the oxygen permeation rate through the oxidized rubber. Thus, the oxidized surface protects the interior of the sample against thermooxidative degradation. This was the case at 150°C for all materials [Figs. 5(a) and 5(b)]. In contrast, the diffusion at 100°C seems to increase with time [Figs. 4(b) and 6(b)]. This may be related to an induction time

[t_i - A1 in Figs. 4(a) and 4(b)] for the oxidative crosslinking at 100°C. Continued aging at 100°C would give a self-limiting aging, as was the case at 150°C. The earlier establishment of an oxidized layer at 150°C due to faster oxygen consumption¹ is also obvious in the crosslink density measurements [see Figs. 4(a) and 5(a)]. That the CT and crosslink density results show less oxidative crosslinking at the surface at 150°C than at 100°C is probably an effect of the area resolution, since the resolution of the crosslink density measurements is not better than 2 mm. The crosslink density of the surface may therefore be more or less influenced by bulk material close to the surface. At 100°C the oxidized layer is thick compared to that at 150°C (Table III). The

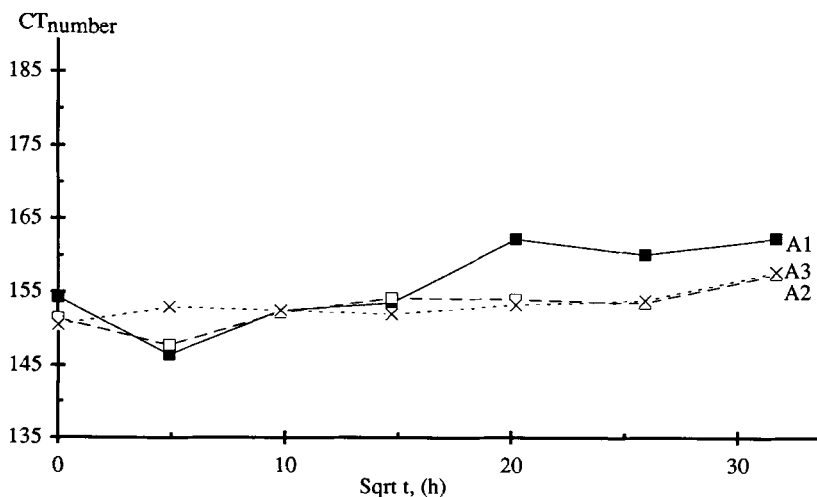


Figure 5(b) CT number of the surface versus the square root of aging time. Materials A1, A2, and A3 aged at 150°C.

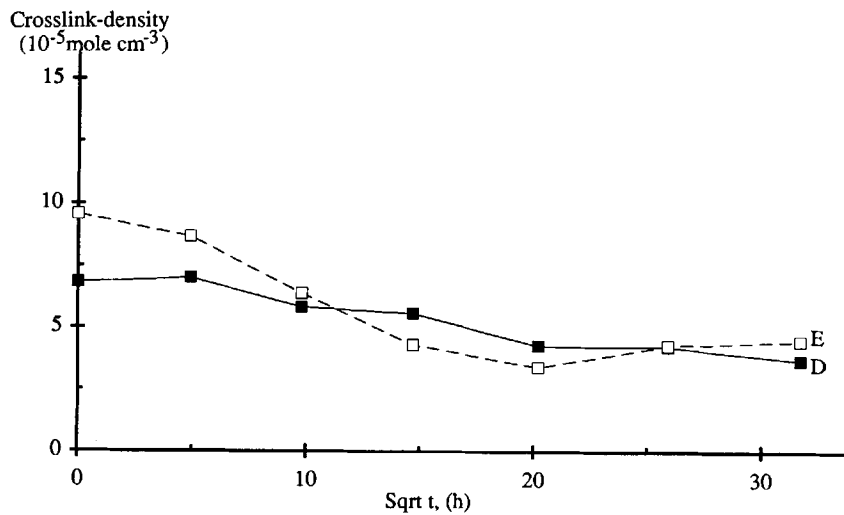


Figure 6(a) Crosslink density of the surface versus the square root of aging time. Materials D and E aged at 100°C .

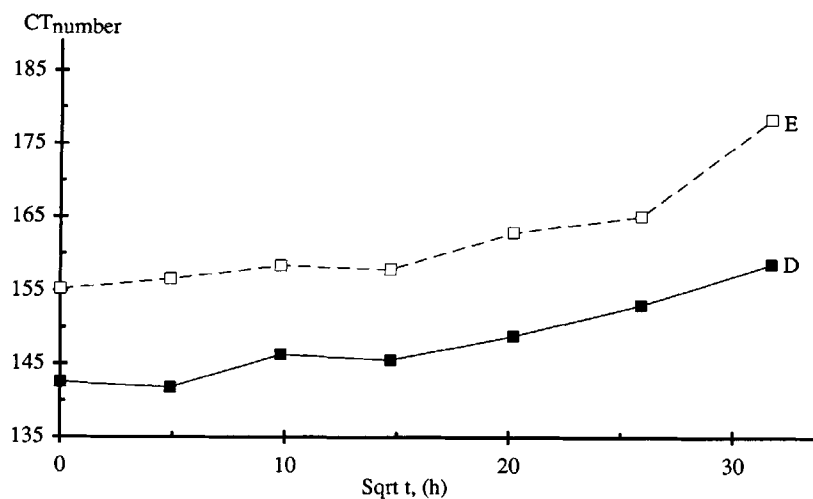


Figure 6(b) CT number of the surface versus the square root of aging time. Materials D and E aged at 100°C .

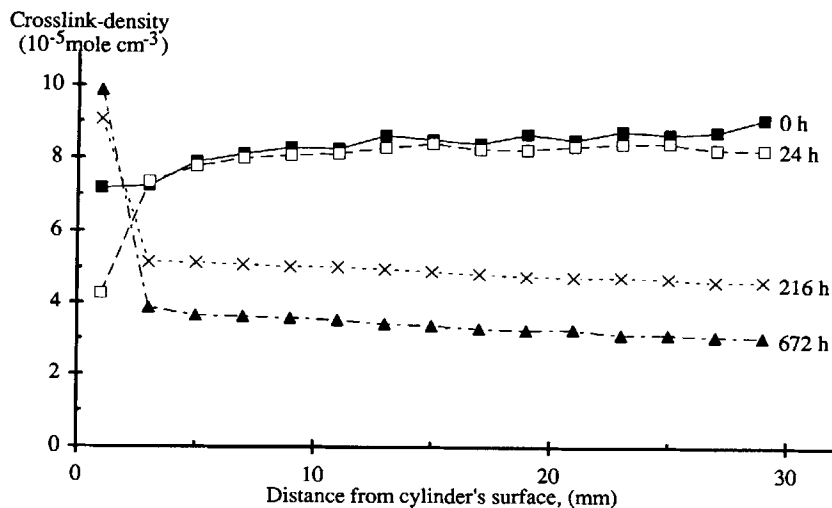


Figure 7 Crosslink density along the radius of material D aged at 150°C at different aging times.

Table III Thickness of Oxidized Layer^a after 1000 h Aging

Material	Temperature		
	70	100	150
	Thickness (mm)		
A1	4.4	2.0	1.4
A2	4.8	2.0	1.2
A3	4.2	2.0	1.0
D	5.4	3.8	1.2 ^b
E	6.0	2.4	1.4 ^c

^a Evaluated from CT measurements.

^b Measured at 672 h.

^c Measured at 408 h.

degraded bulk material close to the surface in 150°C-samples will also lower the measured crosslink density. The low CT number at 150°C is an effect of the diffusion limiting oxidized layer, which is formed at early stages at high temperatures.

A thermal degradation of the network was shown in the bulk of material D aged at 150°C (See Table II). Because of the monosulfidic crosslinks in an EV system the reversion should be low¹⁸ (for this reason EV systems are often used in bulky products and products in need of improved thermal stability). Obviously this was not the case for material D aged at 150°C. It has, however, been indicated¹⁹ that zinc-accelerator complexes promote the degradation of monosulfidic crosslinks. The amount of zinc-accelerator complexes will be much higher in the EV system than in conventional systems, and the EV system will thus be degraded due to zinc-accelerator

complexes to a greater extent than the conventional systems. At shorter times a reversion effect was evident only at the surface, with a reversion in the bulk at longer times (Figure 7). The results obtained by Lindley and Teo²⁰ also show that an EV system has quite a poor resistance towards thermal degradation.

The depth of the oxidized layers decreased with increase in temperature (Table III). This is, as already mentioned, an effect of the self-limiting aging, i.e., faster oxygen consumption at high temperatures and thus earlier formation of layers prevailing from further oxygen diffusion. The reason for the thicker oxidized layer formed in the EV system and in the peroxide system is a greater resistance to oxidative crosslinking, allowing the oxygen to permeate deeper into the bulk of these materials than in the conventional sulfur-vulcanized materials.

Close to the oxidized layer there was an area with a CT number lower than that in the bulk. This was most prominent in material A1 aged at 100°C (Figure 8). This heavily degraded material was soft and tacky, and also seemed slightly porous.

The formation of an oxidized layer at the cylinder surface was also followed visually on the CT images. Because these layers are brittle, there were cracks in the surfaces of material A1, D, and E already after 216 h aging at 150°C. In materials A2 and A3 the antioxidants showed a positive effect, since the cracks did not appear until the cylinders were taken out after 672 and 408 h, respectively, at 150°C. The propagation of the cracks formed in A1, D, and E and the subsequent inner oxidation were easily studied in the CT images [Figs. 9(a)–(d) and 10]. Gas blisters, “black holes”,²⁰ formed during aging could also be detected in these images.

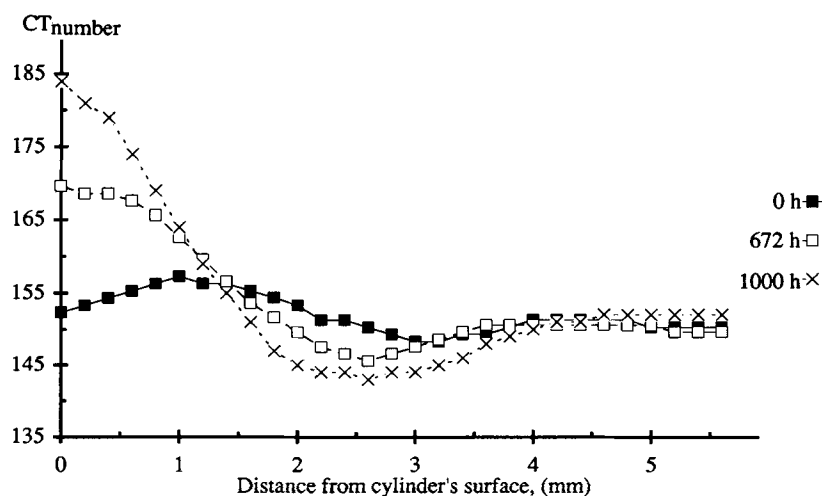
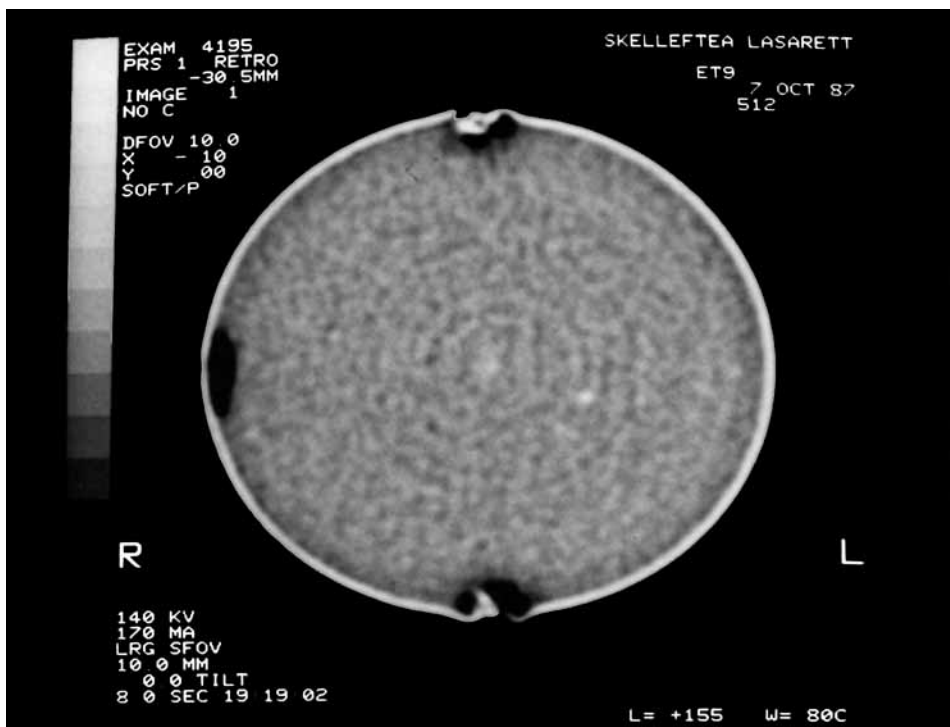


Figure 8 CT number of the outermost rubber in material A1 aged at 100°C at different aging times.



(a)



(b)

Figure 9 CT images of material E aged at 150°C: (a) aged 96 h, (b) aged 216 h, (c) aged 672 h, and (d) 1000 h.

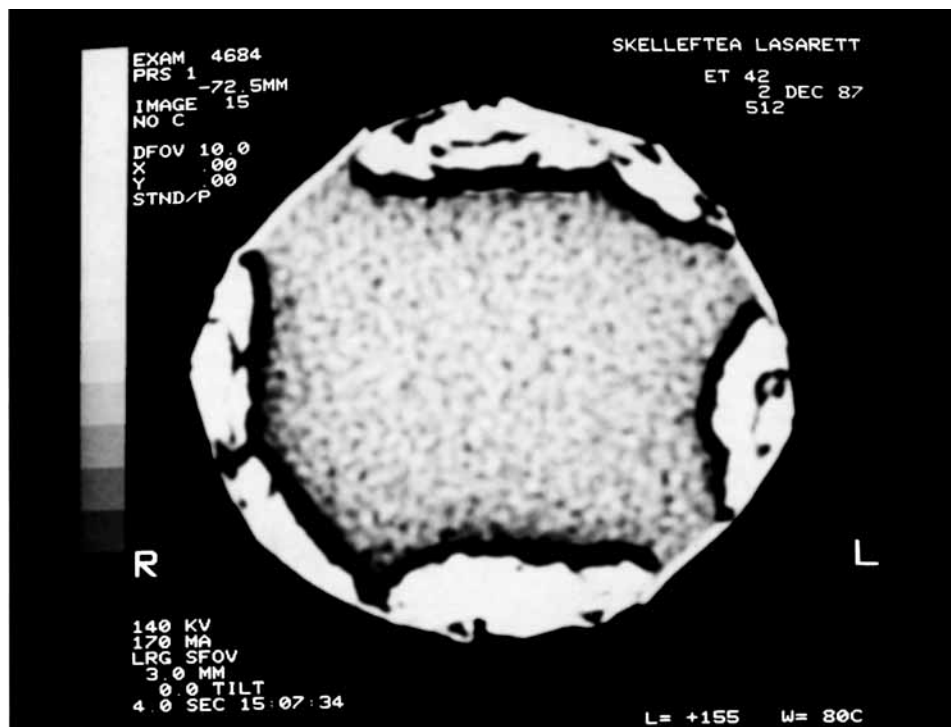
CONCLUSION

The results obtained in this work, where computed X-ray tomography scanning has been used for

thermo-oxidative aging studies, agree with the theory that oxidative aging is limited by the diffusion of oxygen and the rate of oxygen consumption.¹⁶ Since the aged samples were thick-walled, thermal



(c)



(d)

Figure 9 (Continued from the previous page)

degradation of the bulk was thought to be important, at least at 150°C. Surprisingly, thermal degradation was not the dominating factor in the conventional vulcanized materials, while the EV system showed a pronounced reversion of the network in the bulk.

Further CT was shown to be a powerful nondestructive method easily adapted to oxidative aging studies. The formation of an oxidized layer at the surface, cracks in this layer, and propagation of cracks into the bulk can be visually followed on the

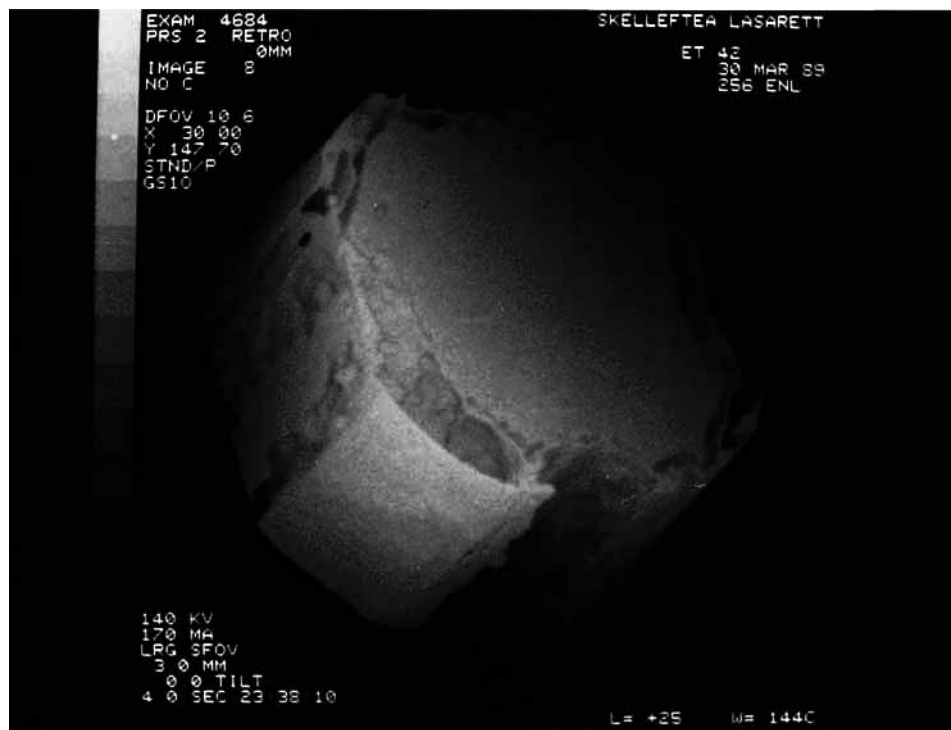


Figure 10 Three-dimensional CT image of material E aged at 150°C.

CT images. The crosslink density changes that occurred during aging could not be detected by CT measurements.

We express our gratitude to the Swedish Board for Technical Development (STU) for financial support.

REFERENCES

1. D. Barnard and P. M. Lewis, in *Natural Rubber Science and Technology*, A. D. Roberts, Ed., Oxford University Press, Oxford, 1988, Chap. 13.
2. P. Mason, *Polymer*, **5**, 625 (1964).
3. K. T. Gillen, R. L. Clough, and N. J. Dhooge, *Polymer*, **27**, 225 (1986).
4. G. N. Hounsfield, *Brit. J. Radiol.*, **46**, 1016 (1973).
5. A. M. Cormack, *J. Appl. Phys.*, **34**, 2722 (1963).
6. A. M. Cormack, *J. Appl. Phys.*, **35**, 2908, (1964).
7. S. Persson, *Polymer*, **29**, 802 (1988).
8. K. D. Fridell, A. R. Lowrey, B. M. Lempiere, and D. W. Cruikshank, Topical Meeting on Industrial Applications of Computed Tomography and NMR. Imaging, MA3, Optical Society of America, 1984.
9. G. M. Bristow and W. F. Watson, *Trans. Faraday Soc.*, **54**, 1731 (1958).
10. L. R. G. Treloar, *The Physics of Rubber Elasticity*, Clarendon Press, Oxford, 1975, Chap. 7.
11. M. Porter, *Kautsch. Gummi, Kunstst.*, **22**, 419 (1969).
12. J. A. Brydson, *Rubber Chemistry*, Applied Science Publ., London, 1978, Chap. 9.
13. A. V. Chapman and M. Porter, in *Natural Rubber Science and Technology*, A. D. Roberts, Ed., Oxford University Press, Oxford, 1988, Chap. 12.
14. B. Mattson, S. Persson, E. Östman, and B. Stenberg, *Rubber Chem. Technol.*, **63**, 23 (1990).
15. G. E. Rogers, in *Polymer Permeability*, J. Comyn, Ed., Elsevier Appl. Sci. Publ., London, 1985, Chap. 2.
16. R. L. Clough and K. T. Gillen, *Polym. Mater. Sci. Eng.*, **58**, 209 (1988).
17. B. Stenberg, Y. J. Shur, and J. F. Jansson, *J. Appl. Polym. Sci. Appl. Polym. Symp.*, **35**, 511 (1979).
18. B. G. Crowther, P. M. Lewis, and C. Metherell, in *Natural Rubber Science and Technology*, A. D. Roberts, Ed., Oxford University Press, Oxford, 1988, Chap. 6.
19. G. P. McSweeney and N. J. Morrison, *Rubber Chem. Technol.*, **56**, 337 (1983).
20. P. B. Lindley and S. C. Teo, *Plastics Rubber: Material Appl.*, **2**, 82 (1977).

Received February 9, 1990

Accepted February 7, 1991